Chapter 18
Crosswind Kite Power with Tower

Florian Bauer, Christoph M. Hackl, Keyue Smedley and Ralph M. Kennel

Abstract   Crosswind kite power replaces the tower and the support structure of a conventional wind turbine by a lightweight tether leading to a potentially lower levelized cost of electricity. However, in this chapter it is shown that tethering the kite to the top of a tower instead of to the ground can have advantages: Most notably, the "cosine loss" is reduced, i.e. the misalignment of the wind velocity vector and the direction of the traction power transfer. Hence, a tower can increase the power and energy yield up to about the double. Even for small tower heights compared to the kite's operation altitude, a significant efficiency increase can be obtained. Further advantages of a tower are highlighted e.g. for the autonomous start and landing and for the wind velocity measurement. Possible tower concepts are illustrated.

18.1 Motivation

Kites, or tethered wings, are promising alternatives to harvest wind energy (see e.g. [1, 5, 11, 20]): As shown in Fig. 18.1, a (rigid) kite is flown in crosswind trajectories resembling figure eights or circles. The kite has onboard turbines and gen-

Florian Bauer (✉) · Ralph M. Kennel
Institute for Electrical Drive Systems and Power Electronics, Technical University of Munich, Arcisstrasse 21, 81477 Munich, Germany
e-mail: florian.bauer@tum.de

Christoph M. Hackl
Research Group "Control of renewable energy systems", Munich School of Engineering, Technical University of Munich, c/o Wind Energy Institute, Boltzmannstrasse 15, 85748 Garching, Germany

Keyue Smedley
The Henry Samueli School of Engineering, Power Electronics Laboratory, University of California, Irvine, CA 92697, USA
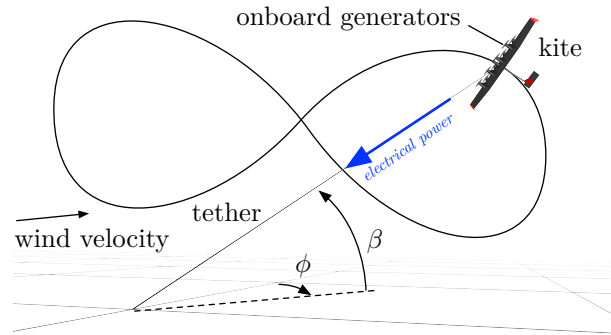
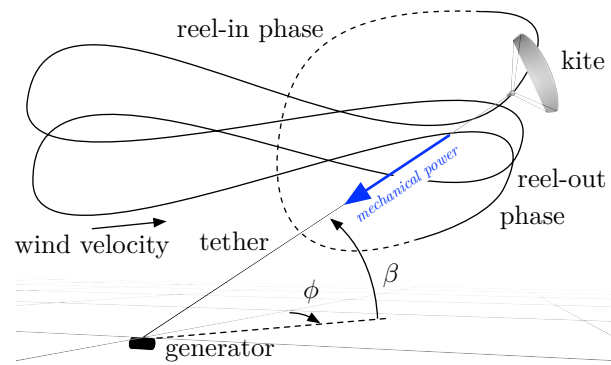**Fig. 18.1** "Drag power": continuous onboard generation of electricity

Fig. 18.2 "Lift power": traction power conversion in periodic pumping cycles by ground-based generator

erators to generate electrical power which is transmitted to the ground via electrical cables that are integrated in the tether. Due to the high speed of the kite, the apparent wind speed at the kite is about a magnitude higher than the actual wind speed, so that the onboard turbines can be small. This concept is called "drag power" [20].[1]

A second possibility for crosswind kite power is shown in Fig. 18.2: A kite (from soft materials like a paraglider or alternatively from rigid materials like a glider) is tethered to a winch on the ground which is connected to an electrical drive. The kite is flown in crosswind motions with a high lift force and pulls the tether from the winch. Energy is generated by operating the winch drive as generator (generative braking). When the maximum tether length is reached, the kite is flown to a low force position like the zenith, and/or pitched down, and reeled back in. A rigid kite can also dive towards the ground winch for minimal reel-in time. During the reel-in

---

[1] Also called "onboard-", "continuous power generation" or "fly-gen".

phase, only a fraction of the generated energy is dissipated by operating the winch drive as motor. This concept is called "lift power" [20].[2]

Both concepts can generate the same amount of power [20]. Compared to conventional wind turbines, crosswind kite power promises to harvest wind energy at higher altitudes with stronger and steadier winds, but by needing only a fraction of the construction material. Hence, it promises to have a higher capacity factor, lower capital investments, and in the end a lower levelized cost of electricity (LCOE). Mechanical output powers of two megawatts have already been achieved by a commercial soft kite by the company SkySails [9]. A drag power rigid kite with a rated electrical power of 600 kW is currently under development by the company Makani Power/Google [21], shown in Fig. 18.3 right.

The power P a kite can generate is proportional to (see also e.g. [22, Eq. (2.38)])

$$P \sim \underbrace{\cos^3 \beta}_{=: \, \eta_{\cos}(\beta)} \tag{18.1}$$

where β is the angle between the wind velocity vector and the direction of the traction power transfer, which is the elevation angle if the tether is assumed straight (see Figs. 18.1–18.2), and $\eta_{\cos}(\beta)$ is the cosine efficiency or $1 - \eta_{\cos}(\beta)$ is the cosine loss. If the kite is tethered to the ground, then $\beta \gg 0$. With a typical elevation of $\beta \approx 30°$, the cosine efficiency is already reduced to $\eta_{\cos}(30°) \approx 0.65$. With $\beta \approx 40°$, as used for Makani Power's/Google's Wing 7 demonstrator [24, p. 486, Table 28.7], the cosine efficiency is only $\eta_{\cos}(40°) \approx 0.45$. Consequently, if the kite is attached to the top of a tower—as proposed in this chapter—, whose height is ideally similar to the operation altitude of the kite, up to $1/\eta_{\cos}(40°) \approx 2.22$ times more power and energy, i.e. more than the *double*, can be generated. Even for smaller towers, the cosine efficiency and thus power and energy yield can be increased significantly. A tower can have further advantages e.g. for the autonomous

Fig. 18.3 Two groups experimenting with towers/masts. Left: TU Delft's demonstrator, provided by Roland Schmehl. Right: Makani Power's/Google's 600 kW prototype [25], reprinted with permission of Fort Felker

---

[2] Also called "traction power", "ground-", "pumping mode power generation" or "ground-gen".
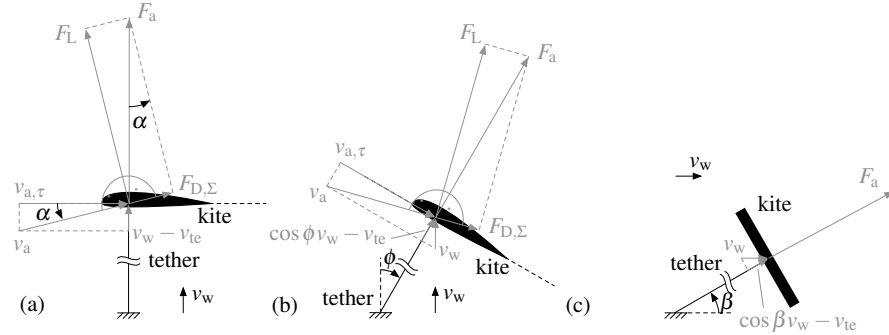
Fig. 18.4 Sketch of a crosswind flying kite from top (a), with azimuth angle $\phi \neq 0$ (b), and seen from the side with elevation angle $\beta \neq 0$ while $\phi = 0$ (c)

start and landing, which is why some groups already experimented with towers, see Fig. 18.3.

The use of a (possibly high) tower is a counter-intuitive approach, as the kite power technology minimizes the construction mass, particularly by avoiding a tower. No publication that details the potentials of a tower was found, so this contribution aims at closing that gap.

This chapter is organized as follows: Section 18.2 derives Eq. (18.1) and reveals the potential of cosine efficiency maximization as function of tether length, tower height and kite operation altitude. Section 18.3 proposes a tower design concept and reveals further advantages of a tower. In Sect. 18.4 the start and landing of a kite from a tower is discussed. Finally, conclusions and an outlook are given in Sect. 18.5.

18.2 Cosine Efficiency and its Maximization

18.2.1 Crosswind Kite Power

The potential of crosswind kite power was first derived by Loyd in [20]. In the following, Loyd's derivation is extended and relies only on the following two assumptions, which are valid for wind speeds above some minimum wind speed and for crosswind flight:

Assumption 18.1: *Gravitational and inertial forces are small compared to aerodynamic forces, i.e. $m_k + m_{te} \approx 0$ with kite mass m_k and tether mass m_{te}.*

Assumption 18.2: *The tether is straight, so that, in combination with Assumption 18.1, aerodynamic force F_a and tether force on ground F_{te} are in balance, i.e. $F_{te} = F_a$, see Fig. 18.4.*

The following derivation of crosswind kite power can partly be found in a similar way e.g. in [1] and references therein.

Figure 18.4 (a) shows a kite flying perpendicular to the wind (i.e. crosswind) when the kite is exactly in the downwind position and the aerodynamic force and the tether force are in balance. One can find the relation

$$\frac{v_\mathrm{w} - v_\mathrm{te}}{v_\mathrm{a}} = \sin\alpha = \frac{F_{\mathrm{D},\Sigma}}{F_\mathrm{a}}, \tag{18.2}$$

where v_w is the wind speed, v_te is the tether speed, v_a is the apparent wind speed, α is the angle of attack and $F_{\mathrm{D},\Sigma}$ is the sum of the drag forces. The aerodynamic forces are determined by

$$F_\mathrm{L} = \frac{1}{2}\rho A v_\mathrm{a}^2 C_\mathrm{L} \tag{18.3}$$

$$F_{\mathrm{D},\Sigma} = \frac{1}{2}\rho A v_\mathrm{a}^2 C_{\mathrm{D},\Sigma} \tag{18.4}$$

$$F_\mathrm{a} = \sqrt{F_\mathrm{L}^2 + F_{\mathrm{D},\Sigma}^2} \tag{18.5}$$

with air density ρ, the kite's characteristic (projected wing-) area A, lift coefficient C_L and drag coefficient sum $C_{\mathrm{D},\Sigma}$. The latter is given by

$$C_{\mathrm{D},\Sigma} = \underbrace{C_{\mathrm{D},\mathrm{k}} + C_{\mathrm{D},\mathrm{te}}}_{=:C_{\mathrm{D},\mathrm{eq}}} + C_{\mathrm{D},\mathrm{tu}} \tag{18.6}$$

with the kite's drag coefficient $C_{\mathrm{D},\mathrm{k}}$, the tether drag coefficient $C_{\mathrm{D},\mathrm{te}}$, which both can be summarized by an equivalent drag coefficient $C_{\mathrm{D},\mathrm{eq}}$, and the "drag" coefficient of onboard turbines $C_{\mathrm{D},\mathrm{tu}}$. All aerodynamic coefficients are in general functions of time. More specifically, C_L and $C_{\mathrm{D},\mathrm{k}}$ depend e.g. on the angle of attack, $C_{\mathrm{D},\mathrm{te}}$ lumps the drag forces of the tether to the kite and depends e.g. on the tether length (see also [15] or [10, Chap. 3.4.1, pp. 44]), and $C_{\mathrm{D},\mathrm{tu}}$ depends e.g. on the angular speed of the turbines. Inserting Eqs. (18.3)–(18.5) into Eq. (18.2) and solving for v_a leads to

$$v_\mathrm{a} = (v_\mathrm{w} - v_\mathrm{te}) \frac{\sqrt{C_\mathrm{L}^2 + C_{\mathrm{D},\Sigma}^2}}{C_{\mathrm{D},\Sigma}}. \tag{18.7}$$

Figure 18.4 (b) shows the same situation as Fig. 18.4 (a) if tether and wind velocity have azimuth $\phi \neq 0$. The vector diagram is similar, but compared to Fig. 18.4 (a) the effect of the wind speed is reduced to $\cos\phi\, v_\mathrm{w}$ leading to a reduced apparent wind speed and kite speed as well as forces. In Fig. 18.4 (c) the situation is shown from the side with an elevation of $\beta \neq 0$ so that, compared to Fig. 18.4 (a), the effect of the wind speed is reduced to $\cos\beta\, v_\mathrm{w}$. Combining both effects, i.e. for arbitrary ϕ and β, leads to the projected wind speed

$$\tilde{v}_{\mathrm{w}} = \cos\phi\cos\beta\, v_{\mathrm{w}}. \tag{18.8}$$

Inserting Eq. (18.8) into Eq. (18.7) gives a "corrected" apparent wind speed (see also e.g. [22, Eq. (2.15)])

$$\tilde{v}_{\mathrm{a}} = (\cos\phi\cos\beta\, v_{\mathrm{w}} - v_{\mathrm{te}})\frac{\sqrt{C_{\mathrm{L}}^2 + C_{\mathrm{D},\Sigma}^2}}{C_{\mathrm{D},\Sigma}}. \tag{18.9}$$

In case of drag power $v_{\mathrm{te}} = 0$ and $C_{\mathrm{D,tu}} \neq 0$. With the turbine's thrust force

$$F_{\mathrm{tu}} = \frac{1}{2}\rho A \tilde{v}_{\mathrm{a}}^2 C_{\mathrm{D,tu}}, \tag{18.10}$$

the power is given by

$$\begin{aligned}
P_{\mathrm{tu}} &= \tilde{v}_{\mathrm{a}} F_{\mathrm{tu}} \\
&= \frac{1}{2}\rho A \cos^3\phi\cos^3\beta\, v_{\mathrm{w}}^3 \frac{\left[C_{\mathrm{L}}^2 + (C_{\mathrm{D,k}} + C_{\mathrm{D,te}} + C_{\mathrm{D,tu}})^2\right]^{\frac{3}{2}}}{(C_{\mathrm{D,k}} + C_{\mathrm{d,t}} + C_{\mathrm{D,tu}})^3} C_{\mathrm{D,tu}}
\end{aligned} \tag{18.11}$$

which contains the proportionality stated in Eq. (18.1).

In case of lift power $v_{\mathrm{te}} \neq 0$ and $C_{\mathrm{D,tu}} = 0$. With $F_{\mathrm{te}} = F_{\mathrm{a}}$, the power for the reel-out phase is given by (see also e.g. [22, Eq. (2.35)])

$$\begin{aligned}
P_{\mathrm{te}} &= v_{\mathrm{te}} F_{\mathrm{te}} \\
&= v_{\mathrm{te}}\frac{1}{2}\rho A(\cos\phi\cos\beta\, v_{\mathrm{w}} - v_{\mathrm{te}})^2 \frac{\left(C_{\mathrm{L}}^2 + C_{\mathrm{D,eq}}^2\right)^{\frac{3}{2}}}{C_{\mathrm{D,eq}}^2}.
\end{aligned} \tag{18.12}$$

By expressing v_{te} in terms of $\tilde{v}_{\mathrm{w}}$ with reeling factor f_{te},

$$v_{\mathrm{te}} = f_{\mathrm{te}}\cos\phi\cos\beta\, v_{\mathrm{w}}, \tag{18.13}$$

Eq. (18.12) can be rewritten as

$$P_{\mathrm{te}} = \frac{1}{2}\rho A \cos^3\phi\cos^3\beta\, v_{\mathrm{w}}^3 f_{\mathrm{te}}(1 - f_{\mathrm{te}})^2 \frac{\left(C_{\mathrm{L}}^2 + C_{\mathrm{D,eq}}^2\right)^{\frac{3}{2}}}{C_{\mathrm{D,eq}}^2} \tag{18.14}$$

which also contains the proportionality stated in Eq. (18.1).

Note that

$$\eta_{\cos}(\beta) = \cos^3\beta \tag{18.15}$$

is a factor in Eqs. (18.11) and (18.14) and holds for any time instant (if Assumptions 18.1–18.2 hold true).

In [6] it is shown that $P \leq \cos\beta F_{te} v_w$ for an arbitrary tethered object and the term $1 - \cos\beta$ is called cosine loss. It is stated: "Fortunately, for moderate angles, the cosine is still close to one, for example the cosine loss is less than 30 % even if the tether goes upwards with an angle of 45 degrees." [6, p. 14] However, as derived above, in crosswind kite power, also the force is proportional to $\cos^2\beta$ leading to Eq. (18.1). Therefore at $45°$ the actual cosine loss is 65 %. In other chapters e.g. [22, 24], the same proportionality as Eq. (18.1) is derived.

For sake of completeness, maximizing Eq. (18.11) over $C_{D,tu}$ or maximizing Eq. (18.14) over f_{te} both yield, with the assumption $C_L \gg C_{D,eq}$, to a maximum power of

$$P_{max} = \frac{2}{27}\rho A \cos^3\phi \cos^3\beta\, v_w^3\, \frac{C_L^3}{C_{D,eq}^2}, \tag{18.16}$$

where respectively $C_{D,tu}^* = \frac{1}{2}C_{D,eq}$ or $f_{te}^* = \frac{1}{3}$ are the optimal arguments [20].

18.2.2 Mean Cosine Efficiency

Figure 18.5 shows a plot of Eq. (18.15) for $\beta \in [-30°, 90°]$. Hereby the region $\underline{\beta} \in [20°, 40°]$ is marked by a bold black line, representative for a mean elevation $\overline{\beta} \approx 30°$, i.e. for a ground-tethered kite, and the region $\beta \in [-10°, 10°]$ is marked by a bold green line, representative for a mean elevation $\overline{\beta} \approx 0$, i.e. for a tower tethered kite where the tower height coincides with the kite's mean operation altitude.

The mean cosine efficiency (i.e. over a complete flight path at a given wind speed) is determined by

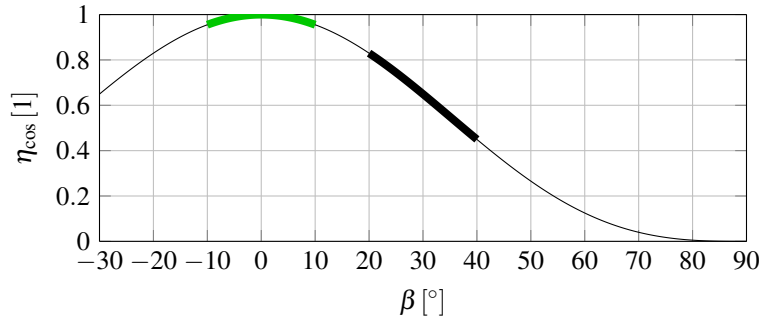$$\overline{\eta}_{cos} := \frac{1}{T} \int_{t_0}^{t_0+T} \eta_{cos}(\beta)\,\mathrm{d}t \tag{18.17}$$

Fig. 18.5 Plot of Eq. (18.15) for $\beta \in [-30°, 90°]$

with initial time t_0 and period time T. Consider that the kite is flown in circles or lying figure eights with $\overline{\beta} - \Delta\beta_{\max} \leq \beta \leq \overline{\beta} + \Delta\beta_{\max}$ with maximum elevation variation due to the flight path of $\Delta\beta_{\max} \approx 10°$ or below. Consider further that the kite's speed is approximately constant. Then the mean elevation (i.e. approximately the elevation of the circle's center or the figure eight's intersection point) is in view of Fig. 18.5 good to estimate $\overline{\eta}_{\cos}$, i.e. the following assumption can be made:

Assumption 18.3:   *The mean cosine efficiency $\overline{\eta}_{\cos}$ can be approximated with the cosine efficiency at mean elevation $\overline{\beta}$,*

$$\overline{\eta}_{\cos} \approx \eta_{\cos}\left(\overline{\beta}\right) = \cos^3 \overline{\beta}. \tag{18.18}$$

In the following, usually mean values are considered.

18.2.3 Cosine Efficiency With Tower

Derived from an initial solution without tower (case A), Fig. 18.6 sketches modified kite power systems (cases B...D). Hereby, $\overline{x}_k$ is the mean horizontal distance, $\overline{h}_k$ is the mean operation altitude of the kite and h_{to} is the tower height. Cases B–D have the following modifications compared to the initial ground-tethered case A:

B: Tower-tethered; $\overline{h}_k$ and $\overline{x}_k$ unchanged, leading to shorter l_{te} and decreased $\overline{\beta}$.
C: Tower-tethered; $\overline{h}_k$ and l_{te} unchanged, leading to larger $\overline{x}_k$ and decreased $\overline{\beta}$.
D: Ground-tethered with longer l_{te} while $\overline{h}_k$ unchanged, leading to a larger $\overline{x}_k$ and decreased $\overline{\beta}$.

In case B, and stronger in case C, $\overline{\beta}$ is decreased and thus $\overline{\eta}_{\cos}$ is increased. A disadvantage of case C compared to case B is the increased $\overline{x}_k$, particularly if a
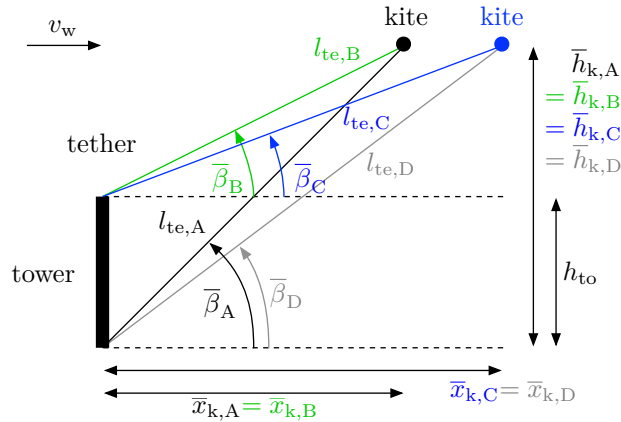

Fig. 18.6 Possible kite power system modifications with a tower or a longer tether

kite power farm or distance restrictions to urban areas are regarded. Moreover, as l_{te} is smaller in case B compared to case C, the mass and drag losses of the tether are reduced (assuming that the tether drag coefficient is proportional to the tether length as in [15]). Case D increases $\overline{\eta}_{cos}$ without a tower while maintaining $\overline{h}_k$, by increasing l_{te}. However, $\overline{x}_k$ and the tether drag and mass losses are increased, and only with $l_{te} \to \infty$ the cosine loss is zero. So this alternative is with limited value, unless a multiple kite system as in [7] is considered, which however would lead to increased complexity and requires further research.

Remark 18.1: *Note that all cases are considered with the same operational altitude $\overline{h}_k$, so that wind shear has no effect on efficiency comparisons. Moreover, as shown in [24, pp. 476], a higher elevation angle is hardly a good choice of tapping stronger winds in higher altitudes for crosswind kite power: "Unless the shear exponent is remarkably high, the best AWT is that which flies at near the minimum practical tether inclination." [24, p. 477]*

Via trigonometric relations, elevation and cosine efficiency are given by

$$\overline{\beta} = \arcsin \frac{\overline{h}_k - h_{to}}{l_{te}} = \arctan \frac{\overline{h}_k - h_{to}}{\overline{x}_k} \tag{18.19}$$

$$\Rightarrow \overline{\eta}_{cos} = \cos^3 \arcsin \frac{\overline{h}_k - h_{to}}{l_{te}} = \cos^3 \arctan \frac{\overline{h}_k - h_{to}}{\overline{x}_k}. \tag{18.20}$$

Obviously, $\overline{\beta} = 0$ and thus $\overline{\eta}_{cos} = 1$ if $\overline{h}_k = h_{to}$.

18.2.4 Numerical Results

Figure 18.7 shows numerical results for increasing tower heights $h_{to} \in [0, \overline{h}_k]$ for two different initial elevations, revealing that $\overline{\eta}_{cos}$ increases almost linearly for small h_{to}. Table 18.1 shows the results for two possible tower heights which are smaller then the operation altitude of the kite: Even if the tower height is only half of the kite's altitude, an efficiency gain of up to 1.89 in case C is possible. If the tower height is only a third of the kite's altitude, still an increase of 1.25 in case B can be achieved. Regarding a mean operation altitude of $\overline{h}_k = 225\,\mathrm{m}$ (as projected for the Makani M600 [14]), the tower heights in the two examples of Table 18.1 are $h_{to} \approx 113\,\mathrm{m}$ or $h_{to} \approx 74\,\mathrm{m}$, respectively. As today's conventional wind turbines have hub heights of up to $\approx 150\,\mathrm{m}$, these figures seem feasible. However, as visualized in Fig. 18.7, a considerable efficiency gain is only achievable if the tower height to operation altitude ratio is not too small. Consequently, the efficiency gain and effectiveness of a tower would be rather low for kite operation altitudes above $\overline{h}_k \approx 1000\,\mathrm{m}$.
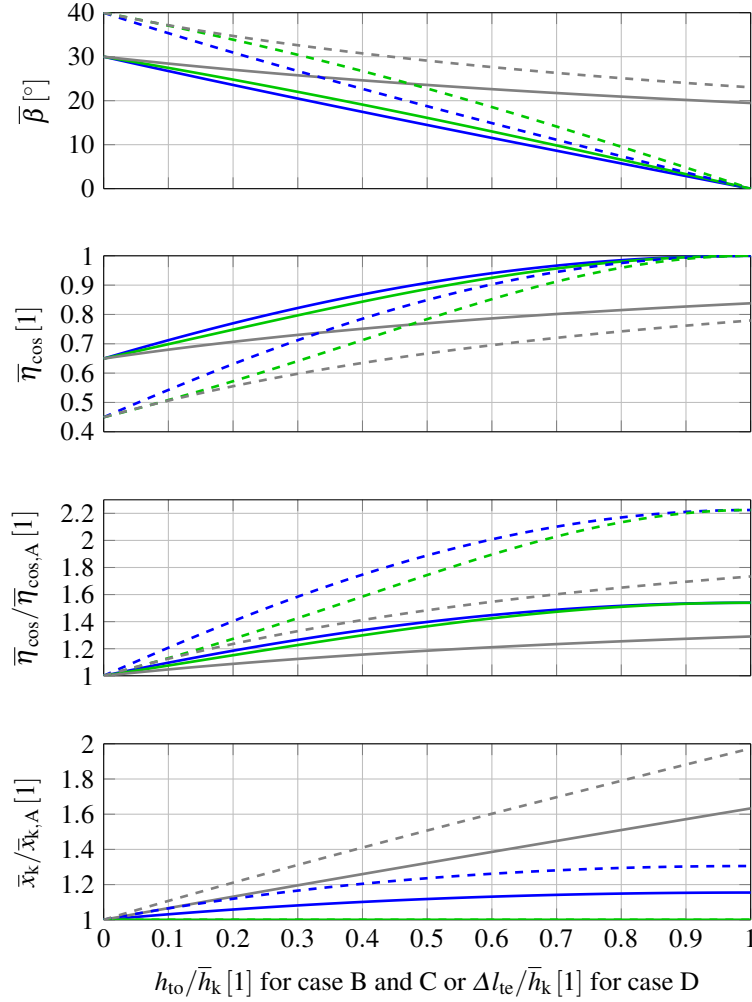
Fig. 18.7 Numerical results for increasing tower heights h_{to} for cases B (——) and C (——), or for increasing tether lengths Δl_{te} for case D (——). From top to bottom: Elevation, cosine efficiency, cosine efficiency gain, horizontal distance normalized to initial horizontal distance. Results for initial elevation $\overline{\beta}_{\text{A}} = 30°$ are drawn-through (——) and for $\overline{\beta}_{\text{A}} = 40°$ are dashed (- - -)

18.2.5 Further Efficiency Increase Effects through a Tower

A tower has further beneficial effects, particularly for drag power where the kite is heavy carrying the generators and the tether is heavy and thick due to integrated cables: As mentioned in Sect. 18.2.3, the tether can be shorter to reach the desired altitude reducing airborne mass and tether drag (assuming that the tether drag coefficient is proportional to the tether length as in [15]). The tether drag reduction

$\frac{h_{\mathrm{to}}}{h_{\mathrm{k}}}$ [1] for cases B and C or $\frac{\Delta l_{\mathrm{te}}}{h_{\mathrm{k}}}$ [1] for case D	case	$\frac{\overline{\eta}_{\cos}}{\overline{\eta}_{\cos,\mathrm{A}}}$ [1] for $\overline{\beta}_{\mathrm{A}} = 30°$	$\frac{\overline{\eta}_{\cos}}{\overline{\eta}_{\cos,\mathrm{A}}}$ [1] for $\overline{\beta}_{\mathrm{A}} = 40°$
	B	1.37	1.74
0.50	C	1.40	1.89
	D	1.19	1.48
	B	1.25	1.47
0.33	C	1.28	1.64
	D	1.13	1.36

Table 18.1 Numerical results for two smaller tower heights for cases B and C, or for increased tether lengths for case D

leads to an increased apparent wind speed which further leads to an increased aerodynamic force, see Eqs. (18.3)–(18.7). As a tower reduces β, the aerodynamic force $F_{\mathrm{a}} \sim \cos^2 \beta$ is additionally increased. All three aforementioned effects can increase the strength to weight ratio $F_{\mathrm{a}}/(m_{\mathrm{k}}g)$ with gravitational acceleration $g = 9.81\,\mathrm{m/s}^2$, leading to a reduced impact of the airborne mass on the efficiency and cut-in wind speed.

18.3 Proposed Tower Concepts

Figure 18.8 illustrates possible tower concepts for different kite power concepts. The proposed tower is a steel framework supported by suspension lines reducing the bending moment absorbed by tower and foundation. In special cases, the suspension lines can absorb the majority of the kite's force. Such a tower can be cost-effective and transported in small parts and mounted on site. Similar to a conventional wind turbine, only a small area is occupied and the area around can be used e.g. for agriculture. Moreover, after its lifetime, such a steel framework tower has a high recyclability. Note, that such a tower concept is not an option for conventional wind turbines, as the rotor disk would intersect with suspension lines, see Fig. 18.9. In crosswind kite power the suspension lines do not intersect with the tether or the kite, even if $\beta \in [-30°, 30°]$ (due to flight path), as the elevation of the suspension lines β_{s} may be designed e.g. $\beta_{\mathrm{s}} > 60°$. Though, a certain safety distance also for transient situations must be considered in a detailed design.

A steel framework tower with suspension lines is also an option for offshore deployment. Figure 18.10 illustrates a possible concept, which could also be simpler than an offshore tower for conventional wind turbines due to the possibility to absorb a major portion of the tower's moments with suspensions lines.

In all cases in Fig. 18.8, the tower top is yawable for wind alignment. For drag power, a vertical winch on the tower top can be used, as pursued by Makani Power/Google. For lift power, the following solutions are imaginable to avoid tether
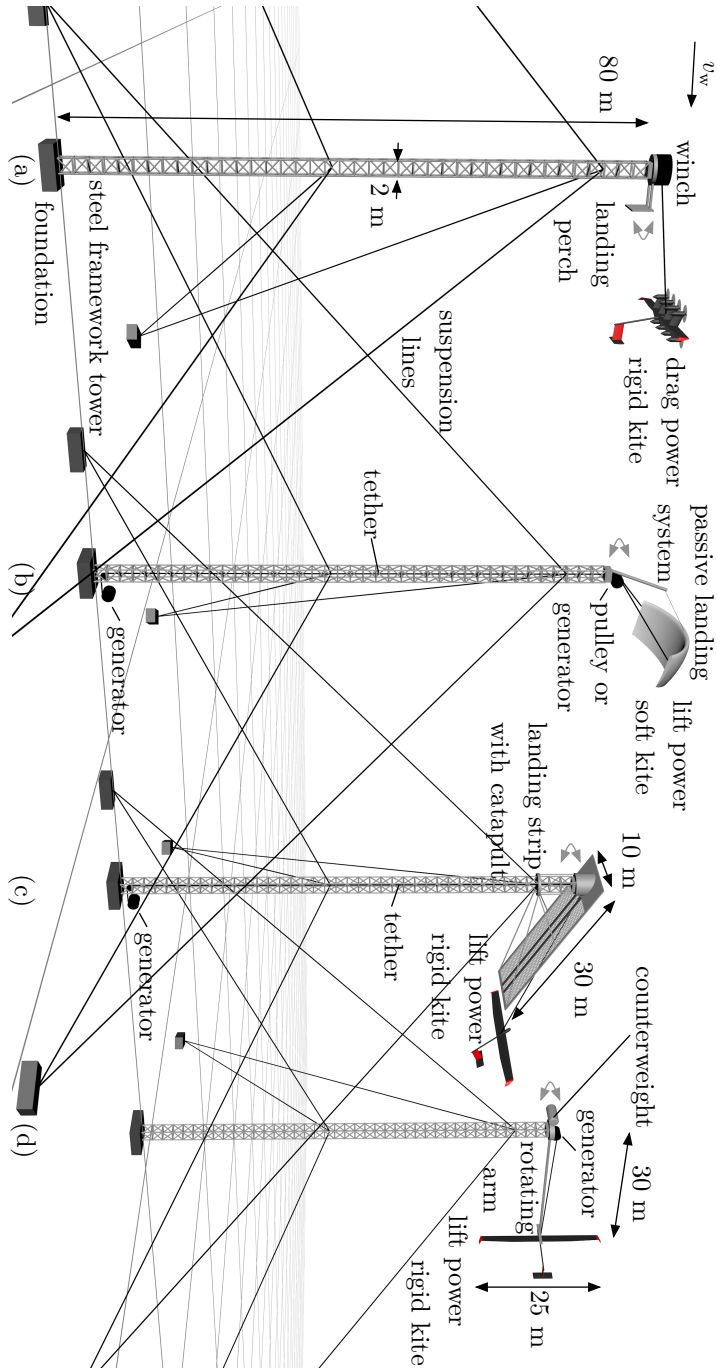
Fig. 18.8 Photomontage of illustrations of proposed steel framework tower with suspension lines for a drag power rigid kite (a), a lift power soft kite with passive start and landing (b), a lift power rigid kite with catapult start and landing strip (c), and a lift power rigid kite with rotating arm start and landing (d)
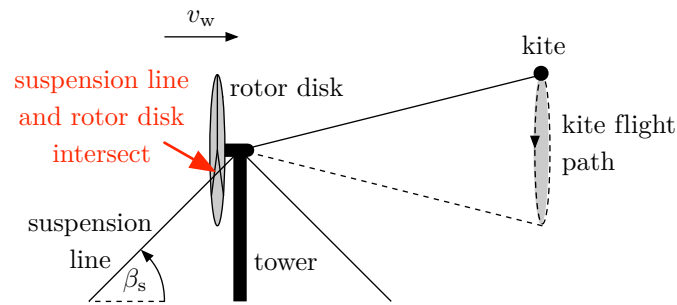
Fig. 18.9 Tower with suspension lines: conventional wind turbine vs. crosswind kite power with tower
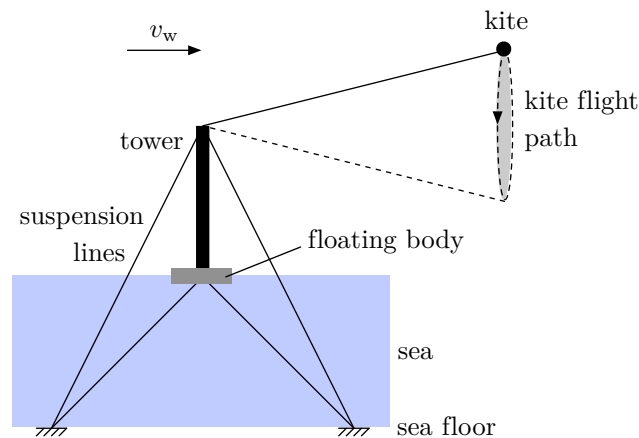

Fig. 18.10 Tower with suspension lines for offshore deployment

twisting during wind alignment: (i) Vertical axis winch with generator on the tower top. (ii) Horizontal axis winch and generator on yawing system on the tower top. (iii) Vertical axis winch and generator inside the tower on ground with a respective tether guidance system. (iv) Horizontal axis winch and generator on ground, pulley system for wind alignment on tower top and tether that allows a twist (inside the tower) of at least $\pm 180°$. (v) Same as (iv) without tether twist, but whole tower with winch and generator on ground is yawable (though probably most expensive and only feasible for small towers). More detailed studies on tether wear and tether guidance are required to evaluate the best solution for lift power.

Figure 18.11 depicts the force diagram for a tower for a drag power system with the assumption that the tower only absorbs compression forces. This simplification can be made for an offshore tower on a floating platform, but an onshore tower with foundation would also absorb a portion of the tether force. In this simplified 2D consideration, tower force and suspension line force are given via trigonometric
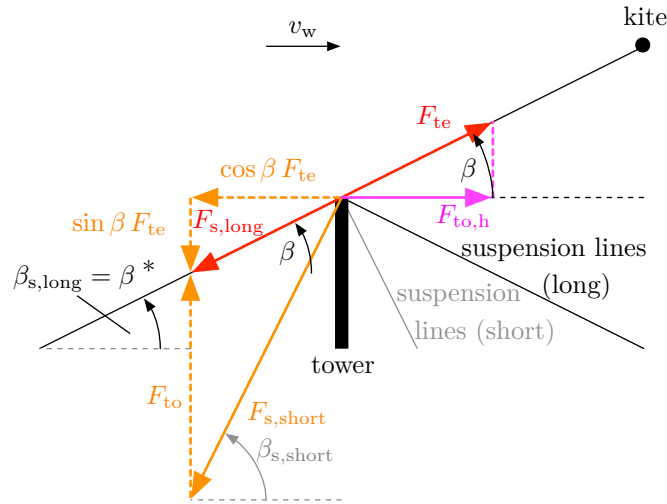
Fig. 18.11 Force distribution with long (red) and short (orange) suspension lines for a drag power system with the assumption that the tower only absorbs compression forces
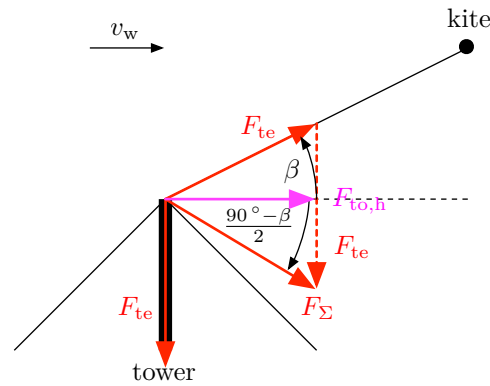

Fig. 18.12 Force distribution for a lift power system with ground-based generator

relations by $F_\text{s} = \cos\beta / \cos\beta_\text{s} F_\text{te}$ and $F_\text{to} = (\tan\beta_\text{s} \cos\beta - \sin\beta)F_\text{te}$. Consequently, the compression force of the tower and the force in the suspension lines increase with the elevation of the suspension lines. For a lift power system, the situation is more complex and unfortunately less beneficial: If the generator is placed on the tower top, the forces are the same as in Fig. 18.11 (with the assumption that the tower only absorbs compression forces), but the generator introduces a torque that tower, suspension lines and foundation have to withstand—this is the torque with which the actual power is generated. It translates either in a bending moment of the tower for a horizontal axis generator or into a twisting moment of the tower for a vertical axis generator. If the generator is placed on ground, a pulley has to direct

the tether force downwards to the generator and leads to a different resultant force which needs to be balanced by tower and suspension lines, as shown in Figure 18.12. In the extreme case of $\beta = 0$, the angle of the resultant force is $45°$ downwards. As the suspension lines also introduce a downward force component, the compression force of the tower can be much higher than compared to Fig. 18.11.

If the elevation angle of suspension lines and kite coincide (superscript * in Fig. 18.11), it might be questioned, why the tower is not replaced by a longer tether. The advantage of the tower of this (unlikely) case would be, that the suspension lines do not move and are not airborne, i.e. they do not contribute to drag nor to the airborne mass and can thus be made cost-efficient from arbitrary materials.

Besides the stated advantages, a tower would have more:

- Autonomous start and landing of the kite is a major challenge, particularly for lift power. This challenge is apparently simplified if the kite is started and landed from a tower, as discussed below in Sect. 18.4.
- Started from the top of the tower, the kite already has a portion of the potential energy of the operation altitude, which reduces energy and time required for the start.
- A wind sensor can be mounted on the tower top. Additionally, several wind sensors can be attached along the height of the tower to allow for a low-cost measurement/estimation of the wind shear and the wind velocity at the kite's altitude. If the wind sensors are mounted on booms similar to a meteorological tower, the measured data would be almost undisturbed, contrary to a conventional wind turbine where a wind sensor is placed on the nacelle behind the rotor. Moreover, as the wind sensors are in upwind direction as seen from the kite, provisions to mitigate gusts (such as the "50-year gust" [4, pp. 214]) can be made and the power output for the near future (magnitude of seconds) can be predicted.
- Another advantage is that a tower allows kite power deployments also in/over forests. If the kite would be anchored to the ground, this would only be possible in a (rather large) cleared area.
- The tower can have additional not kite power-related functions, e.g. a weather station or antennas can be mounted to it.

However a disadvantage is the higher construction mass and costs compared to ground-tethered kites. Moreover, the tower has to withstand about twice the load as a tower of a conventional wind turbine of same power rating: Assume $C_L \gg C_{D,eq}$ and consider the maximum power point $\phi, \beta = 0$. Assume also, that the tower has to withstand only the tether force, so the horizontal tower force is $F_{to,h} = F_{te}$ (see Fig. 18.11 or 18.12). Using the aerodynamic force as given by Eq. (18.3) with apparent wind speed

$$v_a^* = \frac{2C_L}{3C_{D,eq}} v_w \tag{18.21}$$

that occurs at the maximum power as given by Eq. (18.16) [6], the ratio of the horizontal tower force $F_{to,h}$ to the power P is

$$\left(\frac{F_{\text{to,h}}}{P}\right)_{\text{kite}} = \frac{F_{\text{L}}\left(v_{\text{a}} = v_{\text{a}}^*\right)}{P_{\max}} = \frac{\frac{1}{2}\rho A\left(\frac{2}{3}\frac{C_{\text{L}}}{C_{\text{D,eq}}}v_{\text{w}}\right)^2 C_{\text{L}}}{\frac{2}{27}\rho A v_{\text{w}}^3 \frac{C_{\text{L}}^3}{C_{\text{D,eq}}^2}} = \frac{3}{v_{\text{w}}}. \tag{18.22}$$

Thrust and power of a conventional wind turbine (CWT) can be formulated by

$$T_{\text{CWT}} = 2\rho A_{\text{s}} v_{\text{w}}^2 a\left(1 - a\right), \tag{18.23}$$

$$P_{\text{CWT}} = 2\rho A_{\text{s}} v_{\text{w}}^3 a\left(1 - a\right)^2, \tag{18.24}$$

where A_{s} is the swept area and a is the inflow or induction factor [18]. At optimal inflow factor $a^* = \frac{1}{3}$ [18], the horizontal tower force to power ratio is

$$\left(\frac{F_{\text{to,h}}}{P}\right)_{\text{CWT}} = \frac{T_{\text{CWT}}\left(a^* = \frac{1}{3}\right)}{P_{\text{CWT}}\left(a^* = \frac{1}{3}\right)} = \frac{2\rho A_{\text{s}} v_{\text{w}}^2 \frac{1}{3}\left(1 - \frac{1}{3}\right)}{2\rho A_{\text{s}} v_{\text{w}}^3 \frac{1}{3}\left(1 - \frac{1}{3}\right)^2} = \frac{1.5}{v_{\text{w}}} \tag{18.25}$$

which is only half of what the tower for a kite has to withstand (compare with Eq. (18.22)).

Nevertheless, considering a kite power system with $P = 5\,\text{MW}$ at (rated) wind speed of $v_{\text{w}} = 10\,\text{m/s}$, the horizontal tower force is

$$F_{\text{to,h}} = \left(\frac{F_{\text{to,h}}}{P}\right)_{\text{kite}} P = \frac{3}{v_{\text{w}}}P = \frac{3}{10\,\text{m/s}} \times 5\,\text{MW} = 1.5\,\text{MN} \approx 153\,\text{t}. \tag{18.26}$$

Considering that today's cranes can reach more than 100 m height and can lift many hundred tons (see e.g. [19]), it seems possible to design and construct a tower which can withstand the loads of a kite.

18.4 Start and Landing from the Top of a Tower

As mentioned, a tower can have advantages for the autonomous start and landing of the kite. In the following, four major starting and landing concepts are discussed (see Fig. 18.8), with focus on the advantages of the use of a tower.

18.4.1 Drag Power Kites and Vertical Take Off and Landing (VTOL) Lift Power Kites

A drag power (rigid) kite can hover to and from a perch mounted on top of the tower, see Fig. 18.8 (a). Particularly, the kite may have a long tail (if the tower is at least as high as the tail long). Consequently, there is no need for tiltable propellers or a tiltable tail as in [2], which were required if the kite should land on the (flat) ground. This concept is indeed pursued by the company Makani Power/Google [21],

however with a relatively small tower as visible in Fig. 18.3 right. Regarding an operation altitude of $\bar{h}_k \approx 225\,\text{m}$ and tether length $l_{te} = 440\,\text{m}$ (taken from [14] from "M600 Specs"), i.e. $\bar{\beta}_A \approx 30.75°$, and assuming a tower height of $h_{to} = 30\,\text{m}$, the efficiency gain is already $\bar{\eta}_{cos}/\bar{\eta}_{cos,A} \approx 1.13$ (assuming case C in Fig. 18.6) compared to a ground-tethered solution.

If the kite has no tail, as it was pursued by the company Joby Energy [16], the kite could also land on a platform similar to a heliport on top of the tower, or alternatively on ground next to the tower for simpler maintenance from ground.

Similar concepts are also applicable for lift power kites with onboard propellers, which are used for vertical take-off and landing (VTOL) only.

18.4.2 Passive Method for Light (Soft) Lift Power Kites

If a tower is used and the kite is started from the top of the tower, the kite is already exposed to a wind speed that is, depending on the tower height, close to the wind speed of the operation altitude. This allows for a "passive" start and landing just with the help of the wind speed, which is hardly possible if the kite shall be started from ground, due to wind shear. The company SkySails [9, 23] pursues such a concept for offshore applications, which is—with a tower—also possible for onshore sites, see Fig. 18.8 (b).

However, a "passive" concept is only feasible, if the kite is light enough, which is usually the case for soft kites only. The maximum kite mass can be estimated by

$$m_k g \leq F_{L,max} = \frac{1}{2}\rho A v_{w,\text{cut-in},h_{to}}^2 C_{L,max}$$

$$\Leftrightarrow \frac{m_k}{A} \leq \frac{\rho v_{w,\text{cut-in},h_{to}}^2 C_{L,max}}{2g}. \tag{18.27}$$

Regarding a cut-in wind speed at the tower height of $v_{w,\text{cut-in},h_{to}} = 3\,\text{m/s}$, air density $\rho = 1.2\,\text{kg/m}^3$ and a soft kite with maximum lift coefficient of $C_{L,max} = 1$, the result is $m_k/A \leq 0.55\,\text{kg/m}^2$. For $v_{w,\text{cut-in},h_{to}} = 4\,\text{m/s}$ and otherwise identical values, the result is $m_k/A \leq 0.98\,\text{kg/m}^2$.

18.4.3 Catapult-Method for (Rigid) Lift Power Kites

Similar to a fighter jet on an aircraft carrier, a heavier rigid lift power kite can be started in a catapult launch, as pursued e.g. by Ampyx Power [17] or ABB [12]. The kite is launched with a high acceleration powered by the winch or by a catapult technology, such as linear motors (which are also used e.g. for roller coasters). Small onboard propellers may help to climb to the operation altitude. To allow for a short

landing strip, the kite is caught and stopped by the ground winch or an additional braking system such as a hook on the kite and lines on the landing strip.

As shown in Fig. 18.8 (c), a landing strip on a tower can be inclined (quite intensely). Consequently, during launch, the kite is catapulted already with an upward component, instead of purely horizontal. The kite needs to climb to a minimum operation altitude $h_{k,min}$ and minimum operation tether length, i.e. from which it can start to fly crosswind motions and make the remaining way with the wind power. Regarding that the kite has to climb to $h_{k,min}$ alone with the kinetic energy from the catapult, the required start speed $v_{k,start}$ can be approximated by conservation of energy (see also [3, Chap. 4.3])

$$E_{kin,start} = E_{kin,min} + E_{pot,min-op}$$
$$\frac{1}{2}m_k v_{k,start}^2 = \frac{1}{2}m_k v_{k,min}^2 + m_k g(h_{k,min} - h_{to})$$
$$\Leftrightarrow v_{k,start} = \sqrt{v_{k,min}^2 + 2g(h_{k,min} - h_{to})} \qquad (18.28)$$

where $E_{kin,start}$ is the kinetic energy at the end of the catapult, $E_{kin,min}$ is the minimum kinetic energy with speed $v_{k,min}$, and $E_{pot,min-op}$ is the minimum operation potential energy. With acceleration a, the catapult length l_c is given by

$$l_c = \frac{v_{k,start}^2}{2a} = \frac{v_{k,min}^2 + 2g(h_{k,min} - h_{to})}{2a} \qquad (18.29)$$

where Eq. (18.28) is inserted. Taking the requirements of the Ampyx Power-Plane from [3, p. 29, Table 3.1] as example with $v_{k,min} = 22\,m/s$, $a = 50\,m/s^2$, $h_{k,min} = 125\,m$, and the example tower height of $h_{to} = 80\,m$, the catapult (or landing strip-) length has to be only $l_c \approx 13.7\,m$, i.e. less than half as long as sketched in Fig. 18.8 (c). For a 30 m long catapult and otherwise identical values, an altitude of up to $\approx 208\,m$ can be reached. This implies that the kite might not need further measures like propellers for the start.

Concerning the landing, the kite can approach on a low altitude even below the landing strip and is put into a steep climb shortly before touch-down. As a consequence, a portion or the complete kinetic energy of the kite can be converted into potential energy of the kite itself. This effect can be approximated by conservation of energy

$$E_{pot} = m_k g\Delta h = \frac{1}{2}m_k v_{k,min}^2 = E_{kin,min} \qquad (18.30)$$

$$\Leftrightarrow \Delta h = \frac{v_{k,min}^2}{2g} \qquad (18.31)$$

where Δh is the maximum height the kite can climb with its kinetic energy $E_{kin,min}$ at $v_{k,min}$. Regarding that the kite approaches the landing strip with speed $v_{k,min} = 22\,m/s$, the maximum climb height is $\Delta h \approx 25\,m$. Consider Fig. 18.8 (c) with tower height $h_{to} = 80\,m$, landing strip inclination $30°$ and length 30 m, i.e. the landing strip

starts at altitude $\approx 80\,\mathrm{m} - \sin(30°) \times 30\,\mathrm{m} = 65\,\mathrm{m}$. The kite would be stopped by potential energy alone, if it approaches in approximately 55 m altitude or 10 m below the start of the landing strip. This implies that no further braking system might be required.

The tether can help to guide the kite during landing. However, if during approaching e.g. a crosswind gust hits the kite in the situation shown in Fig. 18.8 (c) with the danger of a crash landing, the landing can hardly be aborted with a subsequent retry, especially if the kite has no propeller. One exit of such a situation could be the separation from the tether and an emergency landing on ground. A small rocket engine on the kite (with fuel just for a few seconds) may help to catapult the kite away and avoid a collision with the tower or suspension lines. By any means, the landing strip should be broad enough for a low probability of the need to perform such an emergency landing.

18.4.4 Rotating Arm-Method for Lift Power Kites

Another start and landing method, is the "rotating arm" method [3, 13]: The kite is rotated at the tip of an arm and slowly released. Operation altitude and -tether length are approached with a helix flight path. The landing is (roughly) the reverse motion.

If such a concept is implemented on ground, the kite would need to start with a (very) small roll angle, i.e. the kite's wings are approximately parallel to the ground (otherwise the outer wing would intersect with the ground), which complicates the design and control and may require a long arm. Moreover, the circular area enclosed with the radius of the arm's length plus half of the wing span cannot be accessed and used e.g. for agriculture. To mitigate these problems, the company EnerKite [8] intends to use a telescoping arm to which the kite is attached for the start and the landing, and retracted during power generation.

If the rotating arm is attached to the top of a tower, as illustrated in Fig. 18.8 (d) (which is also similar to [13, Fig. 1.2 (c)]), these disadvantages are not existent: The kite can be attached to the arm with a high roll angle, even up to $90°$, i.e. the wings are parallel to the tower (regarding that the arm is long enough and the elevation of the suspension lines is large enough). The length of the arm has no effect on the occupied ground area. However, the (heavy) generator might need to be placed on the top of the tower and needs to be rotated with the arm to avoid tether twisting during start and landing.

18.5 Conclusions and Outlook

In this chapter, the possible benefits of a tower in crosswind kite power technology are discussed: Although it is a counterintuitive and contrary approach to tether the kite to the top of a tower, as this wind energy technology does not rely on a tower, a

significant efficiency increase can be obtained yielding up to more than the double of the power and energy output compared to a ground-tethered kite. A tower design based on a steel framework and suspension lines is proposed. The advantages of a tower can be summarized as follows:

- Significant increase of cosine efficiency, or decrease of cosine loss almost down to its elimination.
- Decrease of tether drag and mass losses as the tether is shorter to reach the same altitude without increase of horizontal distance.
- Increase of the strength to weight ratio.
- (Apparent) Simplification of start and landing for both, drag power and lift power kites.
- Lower potential energy demand for the start, if the kite is started from the top of the tower.
- Simplified wind velocity measurement/estimation for the kite's altitude.
- Possibility to deploy kite power in/over forests (without the need for a clearing).
- Multi-functionality of the tower, e.g. by adding a weather station or antennas.
- Compared to conventional wind turbines, a simpler and more cost-effective tower seems possible.

However, disadvantages compared to ground-tethered kites include the higher material demand, higher construction costs and higher maintenance costs. As with conventional wind turbines, the tower needs to transmit the induced bending moment to the ground, while a ground-tether kite requires only a lightweight tensile structure.

In a future work, dynamic simulations should be carried out to identify the cosine efficiency and loads on tower and suspension lines more accurately. The results can then be used for a specific tower design. An economical investigation which considers, capital, material, transportation, construction, demolition and recycle costs could then quantify the financial impact of the tower on the LCOE and optimize the tower height for a site. As the tower is not a requirement, it is even possible to build a (higher) tower some time after the start of operation to reduce capital costs. The tower design concept (also e.g. concrete and steel tube towers), and reliable start and landing from the top of the tower, are subject to further studies.

References

1. Ahrens, U., Diehl, M., Schmehl, R. (eds.): Airborne Wind Energy. Green Energy and Technology. Springer, Berlin Heidelberg (2013). doi: 10.1007/978-3-642-39965-7
2. Bevirt, J. B.: Apparatus for generating power using jet stream wind power. US Patent 20,100,032,947, Feb 2010
3. Bontekoe, E.: How to Launch and Retrieve a Tethered Aircraft. M.Sc.Thesis, Delft University of Technology, 2010. http://resolver.tudelft.nl/uuid:0f79480b-e447-4828-b239-9ec6931bc01f

4. Burton, T., Sharpe, D., Jenkins, N., Bossanyi, E.: Wind Energy Handbook. John Wiley & Sons, Ltd, Chichester (2001). doi: 10.1002/0470846062

5. Cherubini, A., Papini, A., Vertechy, R., Fontana, M.: Airborne Wind Energy Systems: A review of the technologies. Renewable and Sustainable Energy Reviews **51**, 1461–1476 (2015). doi: 10.1016/j.rser.2015.07.053

6. Diehl, M.: Airborne Wind Energy: Basic Concepts and Physical Foundations. In: Ahrens, U., Diehl, M., Schmehl, R. (eds.) Airborne Wind Energy, Green Energy and Technology, Chap. 1, pp. 3–22. Springer, Berlin Heidelberg (2013). doi: 10.1007/978-3-642-39965-7_1

7. Diehl, M., Horn, G., Zanon, M.: Multiple Wing Systems – an Alternative to Upscaling? In: Schmehl, R. (ed.). Book of Abstracts of the International Airborne Wind Energy Conference 2015, p. 96, Delft, The Netherlands, 15–16 June 2015. doi: 10.4233/uuid:7df59b79-2c6b-4e30-bd58-8454f493bb09. Presentation video recording available from: https://collegerama.tudelft.nl/Mediasite/Play/1065c6e340d84dc491c15da533ee1a671d

8. Enerkite GmbH. http://www.enerkite.com/. Accessed 14 Jan 2016

9. Erhard, M., Strauch, H.: Control of Towing Kites for Seagoing Vessels. IEEE Transactions on Control Systems Technology **21**(5), 1629–1640 (2013). doi: 10.1109/TCST.2012.2221093

10. Fagiano, L.: Control of tethered airfoils for high-altitude wind energy generation. Ph.D. Thesis, Politecnico di Torino, 2009. http://hdl.handle.net/11311/1006424

11. Fagiano, L., Milanese, M.: Airborne Wind Energy: an overview. In: Proceedings of the 2012 American Control Conference, pp. 3132–3143, Montréal, QC, Canada, 27–29 June 2012. doi: 10.1109/ACC.2012.6314801

12. Fagiano, L., Schnez, S.: The Take-Off of an Airborne Wind Energy System Based on Rigid Wings. In: Schmehl, R. (ed.). Book of Abstracts of the International Airborne Wind Energy Conference 2015, pp. 94–95, Delft, The Netherlands, 15–16 June 2015. doi: 10.4233/uuid:7df59b79-2c6b-4e30-bd58-8454f493bb09. Presentation video recording available from: https://collegerama.tudelft.nl/Mediasite/Play/2ebb3eb4871a49b7ad70560644cb3e2c1d

13. Geebelen, K., Gillis, J.: Modelling and control of rotational start-up phase of tethered aeroplanes for wind energy harvesting. M.Sc.Thesis, KU Leuven, June 2010

14. Hardham, C.: Response to the Federal Aviation Authority. Docket No.: FAA-2011-1279; Notice No. 11-07; Notification for Airborne Wind Energy Systems (AWES), Makani Power, 7 Feb 2012. https://www.regulations.gov/#!documentDetail;D=FAA-2011-1279-0014

15. Houska, B., Diehl, M.: Optimal control for power generating kites. In: Proceedings of the 9th European Control Conference, pp. 3560–3567, Kos, Greece, 2–5 July 2007

16. Joby Energy. http://www.jobyenergy.com/. Accessed 14 Jan 2016

17. Kruijff, M., Ruiterkamp, R.: Status and Development Plan of the PowerPlane of Ampyx Power. In: Schmehl, R. (ed.). Book of Abstracts of the International Airborne Wind Energy Conference 2015, pp. 18–21, Delft, The Netherlands, 15–16 June 2015. doi: 10.4233/uuid:7df59b79-2c6b-4e30-bd58-8454f493bb09. Presentation video recording available from: https://collegerama.tudelft.nl/Mediasite/Play/2e1f967767d541b1b1f2c912e8eff7df1d

18. Kulunk, E.: Aerodynamics of Wind Turbines. INTECH Open Access Publisher (2011). doi: 10.5772/17854

19. Liebherr GmbH: Lattice boom mobile crane LG 1750. http://www.liebherr.com/en/deu/products/mobile-and-crawler-cranes/mobile-cranes/lg-lattice-mast-cranes/details/lg1750.html. Accessed 14 Jan 2016

20. Loyd, M. L.: Crosswind kite power. Journal of Energy **4**(3), 106–111 (1980). doi: 10.2514/3.48021

21. Makani Power/Google. http://www.google.com/makani. Accessed 14 Jan 2016

22. Schmehl, R., Noom, M., Vlugt, R. van der: Traction Power Generation with Tethered Wings. In: Ahrens, U., Diehl, M., Schmehl, R. (eds.) Airborne Wind Energy, Green Energy and Technology, Chap. 2, pp. 23–45. Springer, Berlin Heidelberg (2013). doi: 10.1007/978-3-642-39965-7_2

23. Skysails GmbH. http://www.skysails.info. Accessed 14 Jan 2016

24. Vander Lind, D.: Analysis and Flight Test Validation of High Performance Airborne Wind Turbines. In: Ahrens, U., Diehl, M., Schmehl, R. (eds.) Airborne Wind Energy, Green Energy

and Technology, Chap. 28, pp. 473–490. Springer, Berlin Heidelberg (2013). doi: 10.1007/978-3-642-39965-7_28

25. Vander Lind, D.: Developing a 600 kW Airborne Wind Turbine. In: Schmehl, R. (ed.). Book of abstracts of the International Airborne Wind Energy Conference 2015, pp. 14–17, Delft, The Netherlands, 15–16 June 2015. doi: 10.4233/uuid:7df59b79-2c6b-4e30-bd58-8454f493bb09. Presentation video recording available from: https://collegerama.tudelft.nl/Mediasite/Play/639f1661d28e483cb75a9a8bdedce6f11d